Molecular dynamics simulations of mixed micelles modeling human bile

Marrink, Siewert; Mark, A.E.

Link to publication in University of Groningen/UMCG research database

Molecular Dynamics Simulations of Mixed Micelles Modeling Human Bile[†]

S. J. Marrink* and A. E. Mark

Department of Biophysical Chemistry, University of Groningen, Nijenborgh 4, 9747 AG Groningen, The Netherlands

Received July 27, 2001; Revised Manuscript Received December 21, 2001

ABSTRACT: Extensive molecular dynamics (MD) simulations of binary systems of phospholipids and bile salts, a model for human bile, have been performed. Recent progress in hardware and software development allows simulation of the spontaneous aggregation of the constituents into small mixed micelles, in agreement with experimental observations. The MD simulations reveal the structure of these micelles at atomic detail. The phospholipids are packed radially with their headgroups at the surface and the hydrophobic tails pointing toward the micellar center. The bile salts act as wedges between the phospholipid headgroups, with their hydrophilic sides exposed to the aqueous environment. The structure of the micelles strongly resembles the previously proposed radial shell model. Simulations including small fractions of cholesterol reveal how cholesterol is solubilized inside these mixed micelles without changing their overall structure.

Concentrated solutions of long-chain phosphatidylcholine (PC)[1] lipids and bile salts (BS) are commonly used as model systems for human bile. The detergent bile salts solubilize the nonsoluble phospholipids into small mixed micelles. This process is essential for the biological role of bile, which is to transport lipids from the liver to the intestine in order to solubilize digestion products and to help eliminate cholesterol from the body. Although the size and composition of these micelles can be studied experimentally, the mutual packing of the components inside the micelles eludes experimental determination so far. Essentially two models have been proposed in the literature: the stacked disk model and the radial shell model. They are pictured schematically in Figure 1.

The models differ in the way the phospholipids are oriented, but both can account for the experimental observation that the mixed micelles turn into rodlike micelles when the ratio of PC/BS is increased. The stacked disk model was originally proposed by Shankland (*1*), on the basis of the mixed disk model of Small (*2*). It assumes the phospholipids are packed parallel to the rod axis into small bilayer patches surrounded by bile salts. In their version of the mixed disk model, Mazer et al. (*3*) suggested that some bile salts might exist as hydrogen-bonded pairs with their steroid parts sticking into the bilayer. In the radial shell model, introduced by Ulmius et al. (*4*), the phospholipids are oriented radially with respect to the rod axis. The bile salts act as wedges filling the space between the phospholipid headgroups and could be arranged with their long axis either parallel [as suggested by Nichols and Ozarowski (*5*)] or, at least partly, perpendicular [in the original model (*4*)] with respect to the rod axis. Recent analysis of scattering data obtained during micellar growth in model bile systems (*6, 7*) appears to be
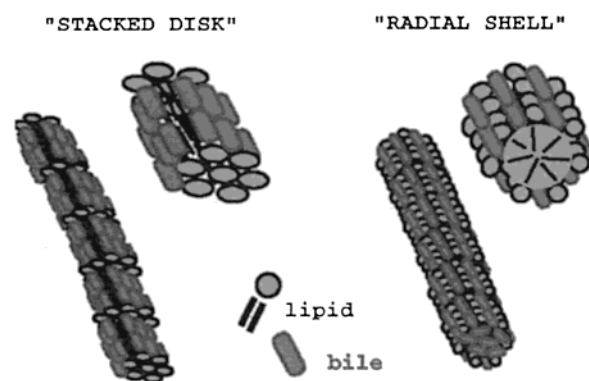

FIGURE 1: Schematic picture of two models for the internal structure of mixed micelles. The stacked disk model assumes a parallel orientation of the phospholipids, whereas the radial shell model assumes a radial orientation. Also shown are the suggested mechanisms by which the micelles can grow into rodlike aggregates.

consistent with the radial shell model as opposed to the stacked disk model. Another important aspect of human bile is its ability to solubilize small amounts of cholesterol (i.e., small with respect to the amount of cholesterol in phospholipid membranes but still large compared to the solubility of cholesterol in water). When cholesterol levels are too high, cholesterol crystals may nucleate [via intermediate liquid crystalline phases (*8, 9*)], forming structures that are precursors to gallstone formation. Experimental studies of PC−BS−cholesterol mixtures indicate that mixed micelles can solubilize small amounts of cholesterol without changing the properties of the micelles (*9, 10*). The manner in which cholesterol is incorporated at the molecular level is unclear.

To analyze in detail the structure of binary mixed micelles containing PC and BS, and ternary micelles which also contain cholesterol, we have performed three extensive molecular dynamics (MD) simulations. The three simulations differ in the relative amount of PC, BS, and cholesterol and should be considered as a first exploratoration of the complex phase behavior of these mixtures using the MD simulation technique. MD simulations have proven very useful in elucidating the structure of bilayers (for recent reviews see refs *11−13*) and micelles (e.g., refs *14* and *15*) in detail. On
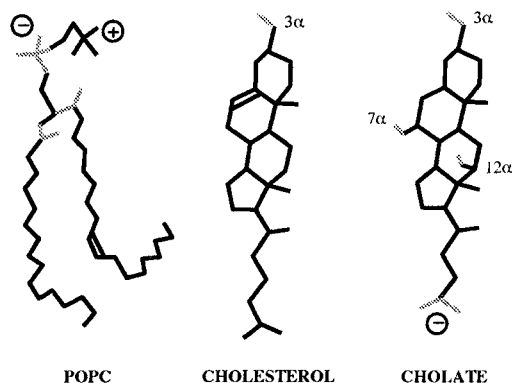
FIGURE 2: Chemical structures of the molecules used in the simulations. The numbering of the hydroxyl groups is given explicitly for later reference.

the basis of simple pairwise interactions such as electrostatic and van der Waals, Newton's equations of motion are solved for a set of particles. From the resulting time trajectory of the system, both structural and dynamical data can be obtained. To avoid biasing the final structure of the micelles, the simulations were initiated from random mixtures of the constituents from which micelles spontaneously self-assemble. This approach follows from recent studies in which we have shown that surfactants spontaneously aggregate into micelles (*16*) and phospholipids into bilayers (*17*) on time scales currently accessible to MD simulations. The simulations presented in this paper are nevertheless still very time-consuming, requiring about half a year of computer power on the currently fastest multiprocessor machines.

The remainder of the paper is organized as follows. In the next section is described the methodology used to perform the simulations, including details of the composition of the systems simulated. This is followed by the presentation of the results, in which the structure of the mixed micelles is analyzed on both a global and a local level. Results on the overall diffusional behavior and of the interior dynamics of the micelles are also presented. The results are then discussed within the framework of the existing literature models.

METHODS

Composition. Experimentally (e.g., refs *3*, *6*, *10*, and *18*), small mixed micelles are observed to form in aqueous mixtures of various PC lipids (such as egg yolk PC and DPPC), with a variety of bile salts (cholate, taurocholate, glycocholate, and their chenodeoxycholate analogues are most frequently used). These micelles have similar properties independent of the exact chemical nature of the constituents. Even replacement of the phospholipids by, for example, monoolein (*7*) or of the bile salts by, for example, octyl glucoside (*6*) results in similar structures. In the simulations palmitoyloleoylphosphatidylcholine (POPC) was chosen as a representative phospholipid of egg yolk PC. It is monounsaturated at the *sn*-2 chain, which is common for the PC lipids found in human bile. The bile salt chosen for the simulations is cholate ($3\alpha,7\alpha,12\alpha$-trihydroxy-5β-cholanoate). The chemical structures of these compounds are shown in Figure 2.

The total concentration of phospholipids and bile salts was set to 10 g/dL and the salt concentration to 0.15 M NaCl. This composition models human gall bladder bile at physi-

ological conditions. The cholate−egg yolk PC−water phase diagram has been studied experimentally by the groups of Small (*19*, *20*) and Carey (*6*, *21*). Mixtures of cholate and egg yolk PC form mixed micelles at concentrations above the CMC of cholate [0.3 g/dL at 0.15 M NaCl (*22*)], at conditions well above the pK_a of cholate [∼5.5 (*23*)] and for PC/BS ratio's larger than 0.5. At lower PC/BS ratio's a phase region is entered with simple bile salt micelles coexisting with mixed micelles. Increasing the ratio of PC/BS results in an elongation of the micelles into rodlike micelles and eventually to the system forming hexagonal and lamellar phases (*6*). The same effect is achieved upon dilution as the micelles become more enriched in phospholipids due to the migration of the highly soluble bile salts into the aqueous phase. At the concentration used in our studies the amount of bile salts in solution is negligible, and various experimental studies predict small, globular micelles with a hydrodynamic radius of 2.5−3.0 nm (i.e., refs *3*, *6*, *7*, *10*, and *18*). BS−PC−cholesterol phase diagrams (*9*) indicate that small amounts (up to ∼8 mol %) of cholesterol can be solubilized by the mixed micellar phase. The size of the micelles is apparently unaffected by the incorporation of small amounts of cholesterol (*24*).

Ideally, one would like to simulate a system containing a number of micelles in order to obtain an equilibrium size distribution. With the computer power currently available this is not possible, however, and one is restricted to the simulation of single micelles. Assuming a perfectly spherical micelle with a radius of 2.2 nm (somewhat smaller than the hydrodynamic radius) and with an overall density of 1 g/cm^3, we estimate a single micelle at a PC/BS ratio of 0.5 will contain on average 32 bile salt molecules and 16 phospholipid molecules. Together with 13000 water molecules (achieving an overall phospholipid concentration of 10 g/dL) and 40 NaCl ion pairs (0.15 M), plus an additional amount of 32 Na$^+$ counterions to neutralize the negatively charged bile salts, this system will be labeled as "32BS−16PC". Similarly we create system "24BS−24PC" containing 24 bile salt molecules and 24 phospholipid molecules, implying a higher PC/BS ratio of 1.0 at the same overall (salt) concentration. The third system we simulate is obtained from system "32BS−16PC" but replacing four of the bile salts by cholesterol molecules (and removing four of the counterions), resulting in 28 bile salts, 16 phospholipids, and 4 cholesterol (CH) molecules (8 mol %). The ratio of nonsurfactant over surfactant, (PC + CH)/BS ≃ 0.7 for this system which we label "28BS−16PC−4CH".

Simulation Procedure. All simulations were performed using the Gromacs simulation package (v2.0) (*25*). The force field of the POPC lipid molecules is the same as that used previously in the bilayer simulations of Tieleman et al. (*26*). The cholesterol force field was taken from Holtje et al. (*27*). Both phospholipid and cholesterol force fields are based on the Gromos96 force field (*28*). The force field used to describe the bile salt was adapted from that of cholesterol, with the partial charges of the atoms of the hydroxyl groups and of the ionic side chain taken from similar groups in the Gromos96 force field (i.e., retinol and glutamate, respectively). All atoms were modeled explicitly, except for the hydrogens attached to carbon atoms. For these a united atom model was employed. All bond lengths and all angles involving hydrogens were constrained using the LINCS
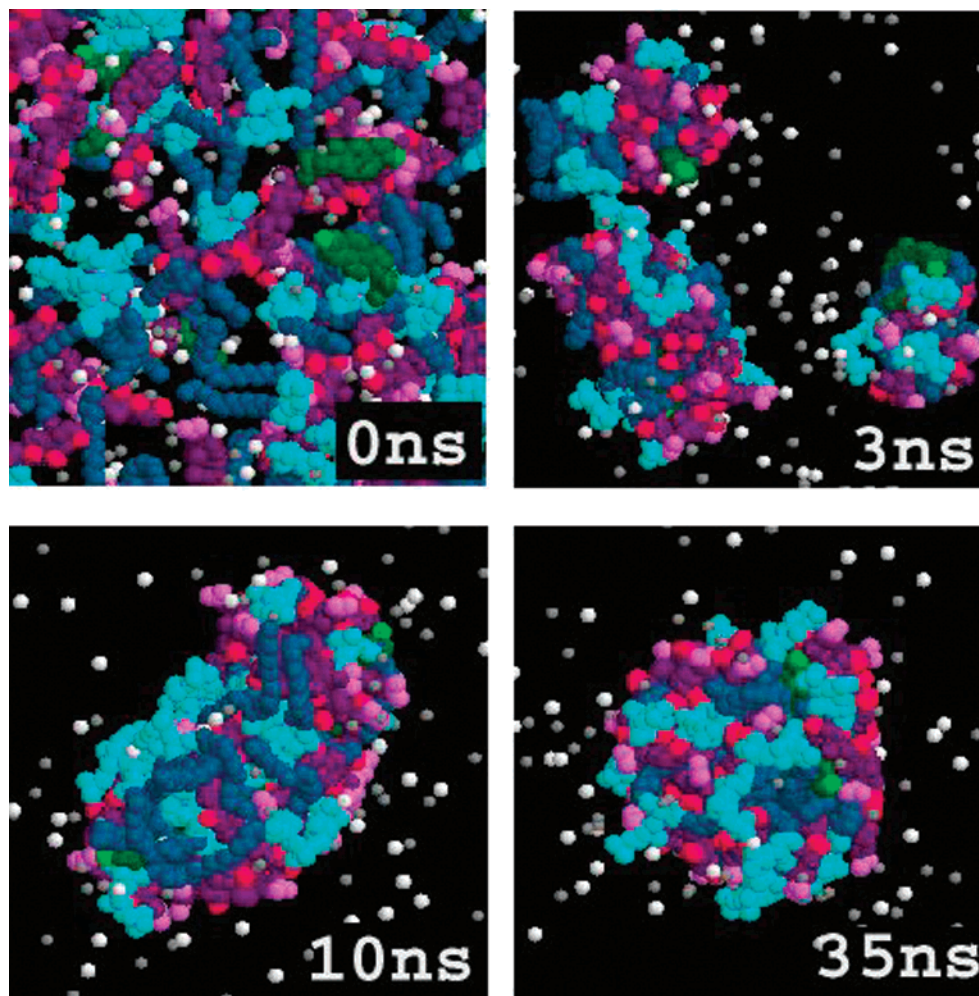
FIGURE 3: Spontaneous aggregation of a random solution of bile salts, singular phospholipids, and cholesterol into a single mixed micelle. Phospholipid headgroups are shown in light blue, phospholipid tails in dark blue, cholesterol in green, and bile salts in purple except for the hydroxyl groups (red) and the ionic group at the chain end (pink). Ions are colored gray (Na^+) and white (Cl^-). Water is omitted for clarity.

algorithm (*29*). The SPC (simple point charge) model was used for the water molecules (*30*). Its geometry was constrained with the SETTLE (*31*) algorithm. The constraining algorithms employed are very stable and permit the use of a 5 fs time step (*32*). A group-based twin range cutoff scheme was used to treat the nonbonded interactions. A cutoff of 1.0 nm was used for the Lennard-Jones and of 1.5 nm for the electrostatic interactions (updated every 5 time steps). Due to the high salt concentration in the systems, long-range electrostatic interactions are effectively screened. This makes the computationally more expensive lattice summation methods unnecessary. [This was explicitly verified by performing an extended simulation of one of the micelles (24BS−24PC) using a significantly larger electrostatic cutoff (1.8 nm), during which no changes in the overall micellar structure were observed.] The system was coupled to a heat bath of 300 K and to an isotropic pressure of 1 atm using standard weak coupling schemes (*33*). Periodic boundary conditions were applied to generate a quasi-infinite solution.

The starting configurations for each of the three systems were generated by randomly placing the constituent molecules inside the cubic simulation box with an initial edge length of 8.6 nm. After energy minimization a short MD run (200 ps) with tight pressure coupling (coupling time 0.1

ps) was performed to allow the overall density of the system to relax. The box size equilibrated to approximately 8.0 nm for each of the three systems. The resulting overall density was close to 1.0 g/dL. Subsequently, a 100 ns simulation was performed for each of the three systems with a pressure coupling of 0.5 ps. Due to the long equilibration times required (see next section), the simulation of system 32BS−16PC was extended to 150 ns. For the analysis of the equilibrium properties of the micelles only the last 50 ns of each of the trajectories was used. Most of the calculations were performed in parallel on a Linux cluster consisting of dual Pentium-800 nodes, achieving a rate of ∼1 ns/24 CPU hours per dual processor node.

RESULTS

Aggregation. The spontaneous aggregation of the molecules into mixed micelles during the simulations is illustrated in Figure 3 for the system 28BS−16PC−4CH. At the start of the simulation, the molecules were placed randomly in the simulation box. Due to the exposure of the hydrophobic parts of the molecules to the aqueous environment, this is a highly unfavorable conformation, and a rapid clustering of the molecules into small micelles (3 ns) was observed. These small micelles are unstable and coalesce to form one large micelle within 10 ns. This micelle appears
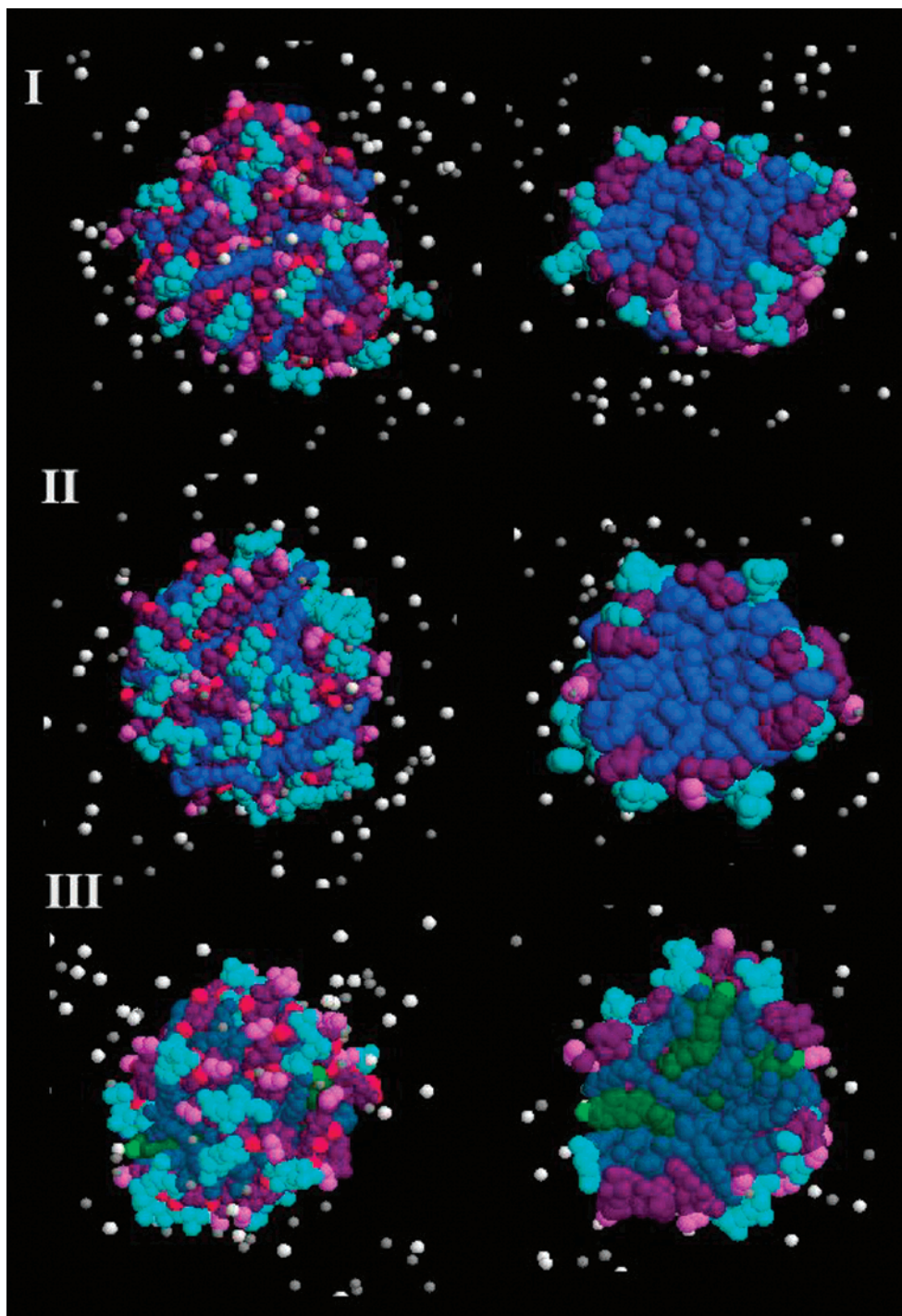
FIGURE 4: Equilibrium structure of the mixed micelles. For each of the three simulated systems representative snapshots of both the outside (left) and the interior (right) of the micelle are shown. For the coloring scheme, see caption of Figure 3.

stable. Nevertheless, the micelle takes a relatively long time (25 ns) to internally reorganize. Initially elongated, the micelle gradually becomes spherical (35 ns) and remains so for the remainder of the simulation (100 ns). The equilibration of the micelle was followed using three criteria: the shape of the micelle (via computation of the principal radii), the total energy of the system, and a comparison of the internal distribution of atoms inside the micelle at different times. Using these criteria, the micelle was considered to be equilibrated after 50 ns. The process of aggregation for system 28BS−16PC−4CH observed above was also observed in the other two systems. It is also similar to the process of spontaneous aggregation of dodecylphosphocho-

line into micelles (*16*): a rapid clustering into small micelles, which merge on a 10−20 ns time scale to form one single micelle. The time required for the micelle to internally equilibrate is relatively long and seems to increase with the amount of bile salt present. The longest equilibration time, 80 ns, was observed for system 32BS−16PC, whereas system 24BS−24PC was already equilibrated within 25 ns. System 28BS−16PC−4CH, with 50 ns equilibration time, was in between. It is possible that the phospholipid fraction acts as a lubricant. The systems with a higher relative concentration of PC reorganize more rapidly. In our subsequent analysis of the equilibrium properties of the micelles only the last 50 ns of the simulation will be considered.
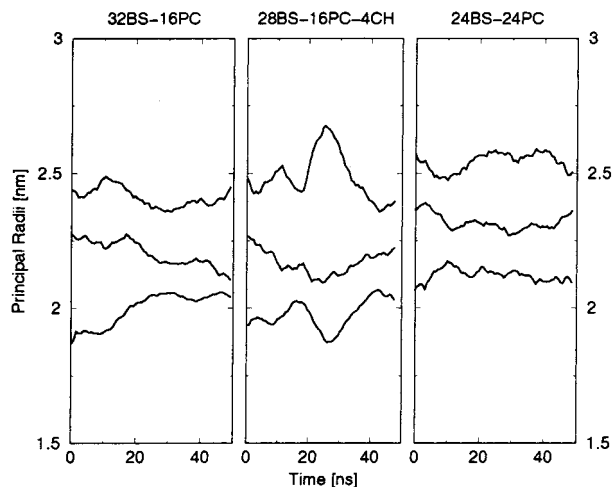
FIGURE 5: Time evolution of the principal radii of the micelles in the three different systems.

Global Structure. Figure 4 shows typical snapshots of the equilibrium structure of the mixed micelles. Cross sections through the micelles are also shown to reveal the interior structure of the mixed micelles. For each of the three different compositions approximately spherical micelles formed. As expected, the surface is occupied by the hydrophilic groups, namely, the phospholipid headgroups and the bile salts. The bile salts have their hydrophilic sides (with the three hydroxyl groups; see Figure 2) and the ionic side chain exposed to the aqueous environment. The interior of the micelle contains predominantly the hydrophobic parts: the phospholipid tails, and in the cholesterol-containing system, the cholesterol body. The distribution of phospholipid headgroups and bile salts across the surfaces is fairly homogeneous. Occasionally, local clustering of bile salts on the surface (more than three adjoining bile salts) is observed during the simulations, but these structures appear only to be short-lived.

Although certainly globular, the micelles do not adopt a perfectly spherical shape. This is best illustrated by the time evolution of the principal radii of the micelles, shown in Figure 5. The longest principal radius is on average about 2.4−2.5 nm for each of the three systems, whereas the shortest radius is about 2.0−2.1 nm. The equilibrium shape of the micelles is thus slightly ellipsoidal. Note, however, due to the flexibility of the micelles, the principal radii continuously change their direction.

Local Structure. Details of the local structure of the micelles are presented in Figure 6, which shows the radial densities of the individual molecules and of some specific functional groups. These densities are computed with respect to the center of mass of the micelle and averaged over the final 50 ns trajectory of the equilibrated systems. Note that the computation of a radial density profile incorporates the nonspherical nature of the micelles in an average way only. Separate analysis of the density distributions along the principal axes, however, revealed no significant differences between the distributions along the short axes and long axes. The micellar distributions can therefore be assumed to be isotropic. The top panel of Figure 6 shows the distribution of the main components in each of the three systems. The overall distribution of bile salts, phospholipids, and water is very similar for the three systems simulated, in agreement with the conclusions drawn from a visual inspection of the
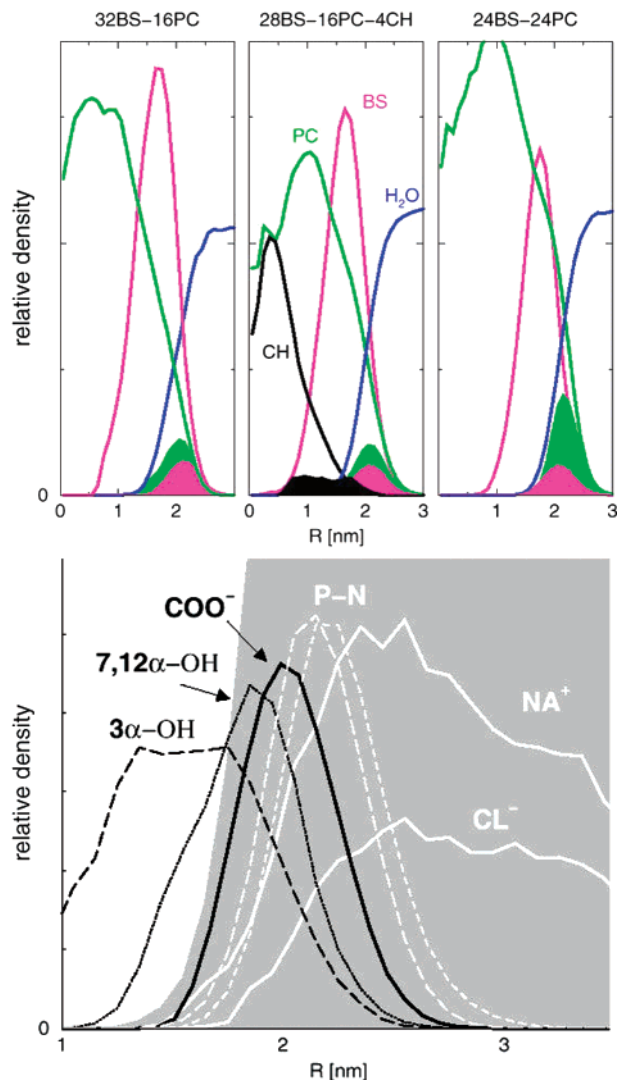

FIGURE 6: Radial density distributions for the various components of the systems with respect to the center of mass of the micelle. Upper: Densities of phospholipid (PC), bile salt (BS), cholesterol (CH), and solvent (H_2O). The distributions of the hydrophilic parts of the phospholipid (i.e., the headgroup), the bile salt (COO^- group), and cholesterol (hydroxyl group) are indicated as filled graphs in the corresponding color. Lower: Detailed distribution of the interfacial region for system 24PC−24BS. The filled area denotes the solvent distribution.

snapshots (Figure 4). It can be clearly seen that the bile salts remain at the surface and never penetrate into the hydrocarbon core. The phospholipid headgroups and the ionic side chain of the bile salt are in direct contact with the water, forming a 1 nm wide interface (the distance over which the water density drops from 90% to 10% of its bulk value). At the micellar core a clear drop in density is observed, which is typical for phospholipid tails in a fluid state. This is also observed in other micellar systems (*14, 15*) and in phospholipid bilayers (*34*) and originates from the entropic repulsion of the tail ends. Only minor differences exist between the three systems. Obviously, due to the larger PC/BS ratio, the relative surface density of bile salts with respect to phospholipid headgroups decreases in the order 32BS−16PC, 28BS−16PC−4CH, and 24BS−24PC. Concomitantly, the width of the distribution of the bile salts is largest for the system with the largest bile salt content, 32BS−16PC, with bile salts penetrating more deeply into the micellar core.

Visual inspection (see Figure 4) shows that occasionally bile salts insert perpendicular rather than parallel to the micellar surface. The cholesterol present in system 28BS−16PC− 4CH is largely solvated in the micellar interior, however, with the hydrophilic hydroxyl group at the surface in contact with water.

The bottom panel of Figure 6 provides more detail on the arrangment of the bile salts, the phospholipid headgroup, and the ions for system 24BS−24PC. The same qualitative features are observed in the other two systems as well. Comparing the distribution of the positively charged nitrogen moiety of the PC headgroup to the phosphorus one, it appears that the distribution of the nitrogen moiety is shifted toward the aqueous phase by a small distance (0.1 nm) only. This indicates that the headgroup dipole is essentially oriented parallel to the surface. Such an orientation is electrostatically most favorable, and the relatively large amount of available surface area in a micelle (pure POPC would form bilayers) does not pose any steric problems for a parallel orientation. The orientation of the bile salt is characterized by the distributions of the hydroxyl groups. The hydroxyls at the 7α and 12α positions have almost identical distributions and are in full contact with the water phase. The 3α-hydroxyl has a broader distribution and spends a considerable time buried more deeply inside the micelle. Apparently, the bile salts do not lie completely flat onto the surface but samples a broader distribution of orientations including more perpendicular ones. The charged acid group, attached to a flexible alkane chain, always remains completely solvated. Due to the negatively charged acid groups, the salt ions form a clear double layer around the micelles, with the sodium ions condensating most closely.

In Figure 7 we show a typical configuration of both a bile salt and a cholesterol molecule surrounded by their neighboring molecules. The bile salt is viewed from the water phase, looking on top of the micellar surface. The bile salt acts like a wedge, filling up the space between of the phospholipid headgroups. The hydrophobic side of the bile salt is faced toward the hydrophobic micellar interior, whereas its hydrophilic side is facing the aqueous phase. Two of the hydroxyl groups are hydrogen bonded to carbonyl groups of the phospholipid glycerol moiety. The third one hydrogen bonds with the solvent. Analysis of the hydrogen-bonding characteristics of the bile salts shows that the hydrogens of the 7α- and 12α-hydroxyls are hydrogen bonded more than 90% of the time, of which roughly 30−40% are to carbonyl oxygens of the phospholipid glycerol moieties, 30−50% to the solvent, and 10−20% to the lipid phosphate oxygens. The ranges indicate the difference between the different systems, with the larger percentage of hydrogen bonds to phospholipids applying to the system with the highest phospholipid ratio (BS24−PC24). These are replaced by hydrogen bonds to the solvent when the PC content decreases. The hydroxyl oxygens can only form hydrogen bonds to the solvent, which they do ∼60% of the time (system independently). Mutual hydrogen bonding between bile salts is rarely observed during any of the simulations (∼1%). For the 3α-hydroxyls the percentages are somewhat different, reflecting their average position further away from the solvent. The percentage of hydrogen bonds both with the solvent and with the phosphate oxygens drops by 10%. These bonds are not replaced with bonds to other groups,
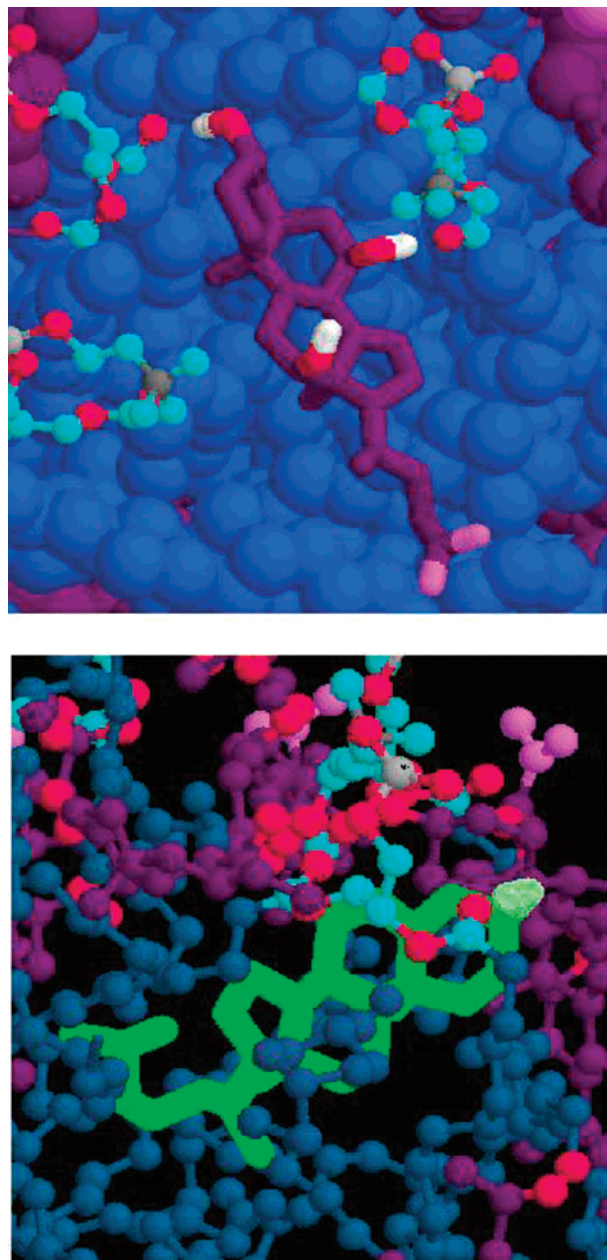

FIGURE 7: Close-up of typical conformations of a bile salt (upper) and of a cholesterol (lower) molecule. For the basic coloring scheme, see caption of Figure 3. Additionally, all oxygens are colored red and hydrogens of the hydroxyl groups white to illustrate the hydrogen bonds.

resulting in an average amount of hydrogen bonds of 70%. The cholesterol hydroxyl acts as a donor during 80% of the time, with equal amounts (30%) to water and phospholipid glycerol. The percentage to the phosphate group is small (5%), but a significant amount of hydrogen bonding is observed with the bile salt hydroxyl groups (15%). Hydrogen bonds between the oxygen of the cholesterol hydroxyl group and water hydrogens are observed 55% of the time. The configuration of cholesterol displayed in Figure 7 is typical, with the steroid body inserted radially into the micelle and the hydroxyl group in the interfacial region hydrogen bonded with a phospholipid carbonyl oxygen. The packing of cholesterol is similar to its packing within phospholipid bilayers, as assessed by a number of recent MD simulations (e.g., refs *35−38*). Although mostly solvated as individual
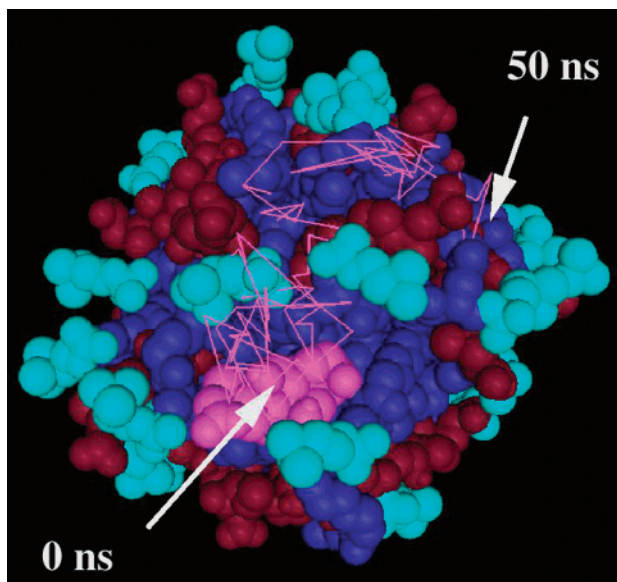
FIGURE 8: Distance covered by a bile salt due to diffusion over the micellar surface in a 50 ns time period. The diffusive pathway for the pink-colored bile salt is shown as a pink trace.

molecules, cholesterol molecules appear to form pairs as well, around 35% of the time. These pairs are found to be quite stable with a typical lifetime of ~10 ns.

Dynamics. The time evolution of the principal radii of the micelles (Figure 5) shows that the micelles are very flexible, especially the systems with a higher BS content. Shape fluctuations in which the radii change by 20% occur on nanosecond time scales. Such fluctuations are a direct consequence of the fluid nature of these micelles and have been also observed in previous simulations of micelles (*14*, *15*).

The diffusional behavior of the micelles can be accessed through evaluation of the mean squared displacement (MSD) of the micellar center of mass over time. For long time scales truly diffusive motion is observed. From the slope of the MSD curve the long time diffusion constant could be obtained for each of the three systems. Within the statistical uncertainty the diffusion constants are equal, $D = 2 \pm 1 \times 10^{-4}$ nm^2 ps^{-1}, and agree with the value predicted from the Stokes–Einstein relation. Using the viscosity of the SPC water model we employed in our simulations ($\eta = 4 \times 10^{-4}$ kg m^{-1} s^{-1}), the Stokes–Einstein relation predicts $D = 1 \times 10^{-4}$ nm^2 ps^{-1} for a (quasi)sphericle particle with a mean hydrodynamic radius of 2.5 nm.

To illustrate the interior dynamics of the micelle, in Figure 8 we show the surface trajectory of an individual bile salt during a time span of 50 ns. The picture was obtained by removing both the translational and rotational diffusion of the center of mass of the micelle. The trace displayed in Figure 8 therefore reflects the relative motion of the individual molecule and is not due to diffusional motions of the whole micelle. A 50 ns time span allows the bile salt to explore only a small part of the micellar surface, but clearly it is not trapped into one location only.

DISCUSSION

Extensive molecular dynamics simulations have been performed on systems modeling human gall bladder bile at physiological conditions. Starting from random binary solu-

tions of phospholipids and bile salts, or ternary solutions also including cholesterol, we observed the spontaneous formation of mixed micelles, in agreement with experiment. The aggregation process occurs on a time scale within 10 ns, relatively fast compared to the internal reorganization of the micelle taking almost an order of magnitude longer. Although the simulation times of the micelles are long compared to current standards, they are still short compared to experiment. In principle, it is therefore possible that the observed equilibrium structures of the micelles are kinetically trapped intermediate structures. Starting from random initial configurations has proven to be an effective way to avoid kinetically trapped intermediate states, however. Spontaneous aggregation into the thermodynamic equilibrium states has been successfully simulated in the case of dodecylphosphocholine [into simple micelles (*16*)] and of phospholipids [into bilayers (*17*)]. The fact that we obtain very similar structures for three independent simulations provides a strong indication that the observed structures represent the thermodynamic ground state.

Comparing the structure of the mixed micelles obtained from the simulations to models that have appeared in the literature (see Figure 1), we find that the radial shell model (*4*) best represents the structure of the aggregates. The phospholipid molecules are oriented radially. The bile salt molecules sit at the surface and fill the space between the phospholipid headgroups. The bile salts are primarily oriented parallel to the surface, in agreement with the proposal of Nichols et al. (*5*). Bile salts do occasionally penetrate into the interior of the micelle but always keep the ionic side chain in the aqueous phase. No evidence for the presence of a population of mutually hydrogen-bonded bile salt pairs was found, as has been suggested (*3*). The phospholipid headgroups protrude into the aqueous phase to a large extent. This allows the phospate–nitrogen dipole to adapt an almost parallel orientation capping the bile salts. The cholesterol is solvated by the phospholipids in a manner similar to that found in phospholipid bilayers. The hydroxyl group is at the interface, and the steroid body is predominantly solvated by the phospholipid chains. Nevertheless, a significant fraction of cholesterol pairs is also observed. As our simulated micelles represent the lower size limit, the micelles are globular rather than wormlike. This might explain the absence of bile salt covered edges as depicted for the radial shell model. Such edges are not likely to be energetically favorable, however, and it is feasible that also the wormlike micelles have spherical ends containing both phospholipids and bile salts. One should bear in mind that the models shown in Figure 1 are highly idealized. At room or physiological temperatures micelles are highly dynamic and liquid-like. They will, therefore, be much more disordered than the idealized models, a feature clearly demonstrated by our simulations.

As mentioned in the methodology section, the simulations described in this paper are limited to a single micelle of predetermined size, which was based on the experimental estimates. Simulations of larger systems are currently being performed that will allow the formation of multiple micelles and mimic the equilibrium size distribution more closely. Simulations of larger systems will also allow us to study the formation of rodlike micelles at increased PC/BS ratio. With growing aggregate size the relative surface area

changes, which might have implications for the packing of the molecules. Whether or not the radial shell model is also favored for larger aggregates remains to be seen. The dependence on the type of bile salt and the amount of cholesterol is also being investigated.

ACKNOWLEDGMENT

REFERENCES

1. Shankland, W. (1970) *Chem. Phys. Lipids 4*, 109−130.
2. Small, D. M. (1967) *Gastroenterology 52*, 607−610.
3. Mazer, N. A., Benedek, G. B., and Carey, M. C. (1980) *Biochemistry 19*, 601−615.
4. Ulmius, J., Lindman, B., Wennerström, H., Johansson, L. B., Fontell, K., Söderman, O., and Arvidson, G. (1982) *Biochemistry 21*, 1553−1560.
5. Nichols, J. W., and Ozarowski, J. (1990) *Biochemistry 29*, 4600−4606.
6. Cohen, D. E., Thurston, G. M., Chamberlin, R. A., Benedek, G. B., and Carey, M. C. (1998) *Biochemistry 37*, 14798−14814.
7. Hjelm, R. P., Schteingart, C. D., Hofmann, A. F., and Thiyagarajan, P. (2000) *J. Phys. Chem. B 104*, 197−211.
8. Wang, D. Q. H., and Carey, M. C. (1996) *J. Lipid Res. 37*, 2539−2549.
9. Gantz, D. L., Wang, D. Q. H., Carey, M. C., and Small, D. M. (1999) *Biophys. J. 76*, 1436−1451.
10. Long, M. A., Kaler, E. W., and Lee, S. P. (1994) *Biophys. J. 67*, 1733−1742.
11. Tieleman, D. P., Marrink, S. J., and Berendsen, H. J. C. (1997) *Biochim. Biophys. Acta 1331*, 235−270.
12. Forrest, L. R., and Sansom, M. S. P. (2000) *Curr. Opin. Struct. Biol. 10*, 174−181.
13. Feller, S. E. (2000) *Curr. Opin. Colloid Interface Sci. 5*, 218−224.
14. Bogusz, S., Venable, R. M., and Pastor, R. W. (2000) *J. Phys. Chem. B 104*, 5462−5470.
15. Tieleman, D. P., van der Spoel, D., and Berendsen, H. J. C. (2000) *J. Phys. Chem. B 104*, 6380−6388.
16. Marrink, S. J., Tieleman, D. P., and Mark, A. E. (2000) *J. Phys. Chem. B 104*, 12165−12173.
17. Marrink, S. J., Lindahl, E., Edholm, O., and Mark, A. E. (2001) *J. Am. Chem. Soc. 123*, 8638−8639.
18. Hjelm, R. P., Thiyagarajan, P., and Alkan-Onyuksel, H. (1992) *J. Phys. Chem. 96*, 8653−8661.
19. Small, D. M., Bourgès, M., and Devichian, D. G. (1966) *Nature 211*, 816−818.
20. Cabral, D. J., and Small, D. M. (1989) in *Handbook of Physiology−The Gastroinstestinal System III* (Schultz, S. G., Forte, J. G., and Rauner, B. B., Eds.) pp 621−662, American Physiological Society, Bethesda, MD.
21. Carey, M. C. (1998) in *Bile Acids in Health and Disease* (Northfield, T. C., Jazrawi, R. P., and Zentler-Munro, P. L., Eds.) pp 61−82, Kluwer Academic Press, Dordrecht, The Netherlands.
22. Carey, M. C. (1985) in *New Comprehensive Biochemistry* (Danielsson, H., and Sjöval, J., Eds.) pp 345−403, Elsevier, Amsterdam, The Netherlands.
23. Small, D. M. (1971) in *The Bile Acids* (Nalr, P., and Kritchevsky, D., Eds.) Vol. 1, p 289, Plenum Press, New York.
24. Mazer, N. A., and Carey, M. C. (1983) *Biochemistry 22*, 426−442.
25. van der Spoel, D., van Buuren, A. R., Apol, E., Meulenhoff, P. J., Tieleman, P. D., Sijbers, A. L. T. M., Hess, B., Feenstra, A. K., van Drunen, R., and Berendsen, H. J. C. (1998) *Gromacs User Manual Version 2.0*, Nijenborgh 4, 9747 AG Groningen, The Netherlands (Internet: http://rugmd.chem.rug.nl/gmx).
26. Tieleman, D. P., Sansom, M. S. P., and Berendsen, H. J. C. (1999) *Biophys. J. 76*, 40−49.
27. Holtje, M., Forster, T., Brandt, B., Engels, T., von Rybinsky, W., and Holtje, H. D. (2001) *Biochim. Biophys. Acta 1511*, 156−167.
28. van Gunsteren, W. F., et al. (1996) *Biomolecular Simulation: The GROMOS96 Manual and User Guide*, Vdf Hochschulverlag AG an der ETH Zürich, Zürich.
29. Hess, B., Bekker, H., Berendsen, H. J. C., and Fraaije, J. G. E. M. (1997) *J. Comput. Chem. 18*, 1463−1472.
30. Berendsen, H. J. C., Postma, J. P. M., van Gunsteren, W. F., and Hermans, J. (1981) Interaction models for water in relation to protein hydration, in *Intermolecular Forces* (Pullman, B., Ed.) pp 331−342, Reidel, Dordrecht, The Netherlands.
31. Miyamoto, S., and Kollman, P. A. (1992) *J. Comput. Chem. 13*, 952−962.
32. Feenstra, A. K., Hess, B., and Berendsen, H. J. C. (1999) *J. Comput. Chem. 20*, 786−798.
33. Berendsen, H. J. C., Postma, J. P. M., van Gunsteren, W. F., DiNola, A., and Haak, J. R. (1984) *J. Chem. Phys. 81*, 3684−3689.
34. Egberts, E., Marrink, S. J., and Berendsen, H. J. C. (1994) *Eur. Biophys. J. 22*, 423−426.
35. Tu, K., Klein, M. L., and Tobias, D. J. (1998) *Biophys. J. 75*, 2147−2156.
36. Smondryev, A. M., and Berkowitz, M. (1999) *Biophys. J. 77*, 2075−2089.
37. Pasenkiewiscz-Gierula, M. Y., Rog, T., Kitamura, K., and Kusumi, A. (2000) *Biophys. J. 78*, 1376−1389.
38. Chiu, S. W., Jakobsson, E., and Scott, H. L. (2001) *Biophys. J. 80*, 1104−1114.